Int J Adv Manuf Technol (2012) 63:523–534
DOI 10.1007/s00170-012-3947-0

ORIGINAL ARTICLE

Development of a special geometry carbide tool for the optimization of vertical turning of martensitic gray cast iron piston rings

G. Severino · E. J. Paiva · J. R. Ferreira · P. P. Balestrassi · A. P. Paiva

Received: 11 November 2011 / Accepted: 19 January 2012 / Published online: 3 February 2012
© Springer-Verlag London Limited 2012

Abstract The machining process for vertical turning martensitic gray cast iron is of great importance to the automotive industry, mainly in the manufacturing process of piston rings. The aim of this paper is to demonstrate the process of development of coated carbide tools to maximize the productivity of the process, considering the maximum life of the cutting tool and the minimum machining cost per part. Using full-factorial design of experiments, we tested two different geometries: a square tool with special geometry—formed by two edges and two ends simultaneously cutting—and a hexagonal tool. Considering that the special square geometry provided maximum life, full quadratic models for responses of interest were constructed using a central composite design for feed (f) and rotation (n). Applying the generalized reduced gradient algorithm, the proposed optimization goals were achieved with feed f=0.37 mm/v and rotation of 264 rpm for the use of the special square tool. Confirmation experiments prove the effectiveness of this solution.

Electronic supplementary material The online version of this article (doi:10.1007/s00170-012-3947-0) contains supplementary material, which is available to authorized users.

G. Severino · E. J. Paiva · J. R. Ferreira · P. P. Balestrassi (✉) · A. P. Paiva
Federal University at Itajubá,
Av BPS 1303,
Itajubá, Minas Gerais, Brazil 37500-903
e-mail: pedro@unifei.edu.br

G. Severino
e-mail: geremias.severino@yahoo.com.br

E. J. Paiva
e-mail: emersonjpaiva@gmail.com

J. R. Ferreira
e-mail: jorofe@unifei.edu.br

A. P. Paiva
e-mail: andersonppaiva@unifei.com.br

Keywords Double vertical turning · Piston rings · Martensitic gray cast iron · Special cutting geometry · Optimization

1 Introduction

The vertical turning of Martensitic cast iron piston rings is a relatively complex machining process. A roughing operation, it is conducted simultaneously on the outer and inner diameters of the parts. Machining is carried out using two twin cutting tools with special geometry; abundant cooling is provided throughout the cutting process. Of the many types of cast iron used by the auto industry, gray cast iron, according to Wang et al. [20], is used most. The main features of gray cast iron are its low melting point [16], good fluidity, and high resistance to wear [4]. Its chemical composition and metallurgical structure, however, compromise its machinability, according to Souza et al. [19]. The machinability of martensitic gray cast iron is aided by its chemical composition, which include graphitizing elements. It also includes elements that impair its machinability: carbide-forming elements and hard abrasives, such as niobium, tungsten, vanadium, chromium, titanium, and molybdenum. These are in addition to the martensitic microstructure, an impairment itself to machinability. Alloying elements can be added to martensitic cast iron material to give it better mechanical properties (higher corrosion and wear resistance, wear, tensile and rupture strength). After casting, gray cast iron is subjected to a tempering process. Here forms the extremely hard and brittle martensitic structure. Consequently, the material undergoes a tempering heat treatment, producing the tempered martensitic structure.

What the industry needs is a conditioning process that improves the machinability of martensitic gray cast iron in

vertical turning operations of piston rings. To meet this need, this paper proposes a new tool geometry as well as an optimization of cutting conditions. Our proposals enable martensitic gray cast iron to meet the industry's quality and productivity standards [14].

Regarding machining processes, many studies have investigated the optimization of cutting parameters and tool geometry by employing design of experiments (DOE). This methodology facilitates studying the optimization of many types of machining processes and materials while considering different manufacturing scenarios. Nalbant et al. [11] use Taguchi designs as methodology; Al-Ahmari [1], Horng et al. [5], and Lalwani et al. [8] use response surface methodology (RSM). The objectives of such studies are to increase production rates, reduce machining costs, and improve component quality. Generally, researchers set up a classical experiment to discover relationships between process variables and the output characteristics of machined products. To determine optimum operating conditions, researchers apply a nonlinear optimization algorithm using the equations obtained by experiment as objective functions or constraints.

Noordin et al. [12] evaluated, in the turning process of AISI 1045, the performance of a hard metal tool with multiple layers. To investigate such factors as cutting speed, feed rate, and tool geometry, the researchers utilized RSM. Also utilizing RSM, Courbon et al. [2] investigated the influence of four cutting parameters on ten responses of high-pressure jet-assisted turning of Inconel 718. These responses were clustered in five groups: cutting forces, contact length, chip formation, surface finish, and heat transmitted to the tool. Reddy and Rao [17] used a Taguchi experimental setup along with a genetic algorithm in the optimization process of milling AISI 1045.

Sarma and Dixit [18] applied a full-factorial design to optimize the cutting parameters of the turning process of gray cast iron. The researchers studied the performance of a mixed ceramic tool in the machining of gray cast iron. Using response surface methodology with neural networks, they analyzed the tool life and surface roughness of the parts. Kurt et al. [7] used arrays of Taguchi to optimize the drilling process of Al 2024 alloy. The hole quality parameters were analyzed under different cutting speeds, feed rates, depths of drilling, and types of drill coating. The Taguchi approach to process optimization was validated by their results. To optimize multiple correlated responses in the turning process of AISI 52100 steel, Paiva et al. [13] applied RSM with principal component analysis and generalized reduced gradient (GRG). They adopted the following parameters: cutting speed, feed rate, and depth of cut. They analyzed the following responses: tool life, cost per manufactured part, cutting time, total machining time, roughness, and rate of removal of material. All of these works cited above sought to optimize the machining process through a small but effective number of experiments.

This work represents a confluence of three approaches—efficient experimental arrangements, objective functions and constraints, and nonlinear solution algorithms for gradient methods. In such manner, we propose to optimize the process of vertical turning martensitic cast iron piston rings by combining ideal cutting parameters and tool geometry. The study's aim is to find a machining condition that leads to the maximum life of the cutting tool, a high production rate, and a minimal per part machining cost.

This paper is organized as follows: "Section 2" provides an overview of the vertical turning process with dual tools as it applies to the packet machining of cast iron piston rings. "Section 2" also covers the chemical composition and mechanical properties of this material. "Section 3" details the chemical composition and geometric characteristics of the developed square and hexagonal tools. It goes into the process parameters and the levels used in the tests of machinability. The section also briefly reviews DOE arrangements. "Section 4" presents a statistical analysis of the effects caused by the machining parameters; it presents the obtained models and the results of the optimization methods on the turning process with the square tool. "Section 5" presents the main findings of the study.

2 Process of vertical turning dual piston rings

Cast iron piston rings, manufactured in sand molds, have an extremely rough and abrasive martensitic surface. Its chemical composition consists of graphitizing elements (silicon, nickel, copper), which assist the machinability, and carbide-forming elements, which impair the machinability (Table 1). This material is characterized by a microstructure consisting of graphite shafts and a tempered martensitic matrix (Fig. 1), with an average hardness of 40 HRC. Deviations in shape and excessive surface roughness, both caused by the smelting process, must be corrected for. To do so, rings with diameters of $Ø$=81.60 mm and 1.95 mm in thickness undergo a process of dual vertical turning (Fig. 2a) in packets of 77 units (Fig. 2), kept under constant pressure and aligned with a recess in the internal diameter (Fig. 2c). The packets

Table 1 Chemical composition of martensitic cast iron

%	C	Si	Mn	P	S	Cu	Cr	Ni	Mo	Ti	V	W	Nb
Mean	3.4	4.3	0.85	0.18	0.08	1.15	0.4	1.05	1.5	0.15	0.75	0.8	0.65

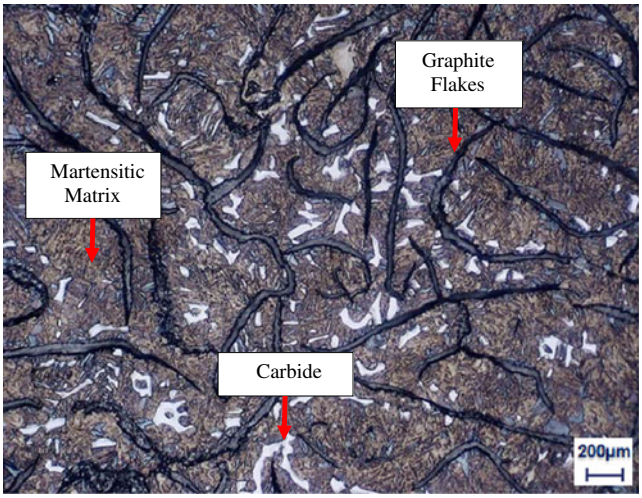

Fig. 1 Tempered martensitic matrix

are drilled vertically by the simultaneous action of two identical, cemented carbide tools.

3 Development of cutting tools

For this work, we designed cutting tools with two geometrical designs: the first was square in shape (Fig. 3a) and the second was hexagonal in shape (Fig. 3b). The cutting tools were made of a twin-carbide substrate ISO class K10, with mechanical properties that are described in Table 2. They were mounted on an indoor and outdoor bar on a vertical lathe. The carbide tips were coated, through a PVD process, with titanium nitride (TiN). For this machining process, we used a CNC vertical lathe, suitable for machining packet rings 150 mm in length in a single machining cycle. The same position angle (Kr) of 45° was used for the internal and external tools.

Table 3 presents the geometrical details of these tools. The basic difference between them is the material removal system (described in Fig. 4). The hexagonal tool was designed with a single-tip radius to remove, in a single pass, 100% of the value determined for the depth of cut (ap). The square tool had two square edges, staggered, with two successive identical end radii that would remove 60% and 40%, respectively, of the material being machined. Since the cutting forces and heat generated are now distributed along two edges, the geometric modification could increase tool life. With the scaling, the tool tip, now having two tip radii, has been strengthened.

3.1 Methodology for the study of the machining conditions

According to the needs of piston ring manufacturers, the ultimate goal of developing new carbide tools coated with TiN is to increase productivity while reducing production costs. Thus, to efficiently test machinability and tool life, we adopted an experimental methodology based on balanced designs [9]. First, a full-factorial design 2^3 was used, adopting as factors: feed (f), rotation (n), and tool geometry (G_t). For the experiment's responses, tool life (T) was adopted, measured in total length machined (mm). For the three cutting parameters, we adopted the experimental levels defined in Table 4. A factorial design is one in which all combinations of k factors in L levels are to undergo experiment; the total number of experiments is equal to $N^k=L$ [3]. At this early stage, there was an experiment with three replicates.

When statistical analysis of the factorial arrangement was carried out, important aspects were found in terms of the adequacy of the tools developed for the process. We were able to determine (a) the geometry that provides the greatest life, (b) the significance of cutting parameters and their more suitable levels for the process, and (c) the interactions between the geometry and the cutting parameters. After defining the best

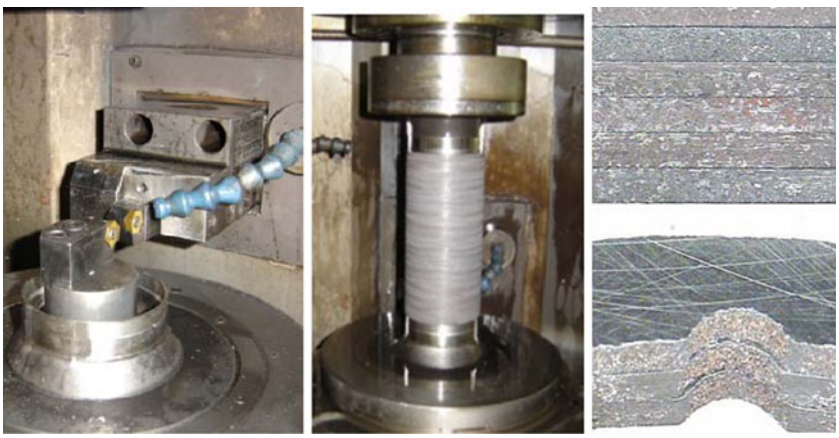

(a) Placement of twin tools (b) Packet with 77 rings (c) internal machining, interrupted cuts

Fig. 2 Vertical turning of Martensitic cast iron piston rings. **a** Placement of twin tools. **b** Packet with 77 rings. **c** Internal machining, interrupted cuts

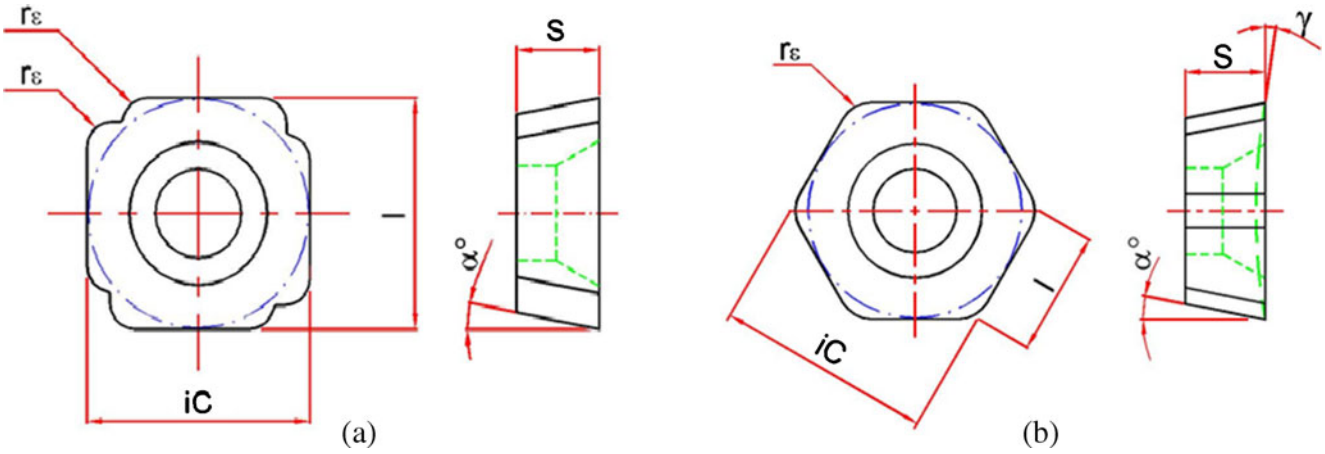

Fig. 3 Square (**a**) and hexagonal (**b**) tools

tool geometry, using an experimental arrangement of the response surface was proposed. An increasing factorial design with axial and central points was built. Doing so allowed the construction of quadratic models for responses of interest. Generally, the points of optimal processes are located in regions near the stationary points of functions.

An arrangement of response surface allows the modeling and analysis of problems in which the response of interest is influenced by a set of variables and in which the response should reach an optimum value [10]. Generally, the relationship between the dependent and independent variables is unknown. For a number of factors generally reduced, it is a reasonable approximation of the real relationship between the responses (**Y**) and the set of independent variables (**x**) [9]. Generally, exploratory experiments have already been performed. Thus, the relationship between variables can be established by a polynomial model such that:

$$\widehat{Y}(\mathbf{x}) = \beta_0 + \sum_{i=1}^{K}\beta_i x_i + \sum_{i=1}^{K}\beta_{ii}x_i^2 + \sum\sum_{i<j}^{K}\beta_{ii}x_i x_j + \varepsilon_\mu = b_0 + \left[\nabla f(\mathbf{x})^T\right] + \left\{\frac{1}{2}\mathbf{x}^T\left[\nabla^2 f(\mathbf{x})\right]\mathbf{x}\right\} \quad (1)$$

In this equation, the parameters (β) of the polynomial are estimated by $\widehat{\beta} = \left(\mathbf{X^T X}\right)^{-1}\left(\mathbf{X^T Y}\right)$. The complete quadratic model shown in algebraic form in Eq. 1 can also be written in matrix form, where **x** is the vector of experimental points, $\left[\nabla f(\mathbf{x})^{\mathbf{T}}\right]$ is the gradient of the function evaluated at **x**, and $[\nabla^2 f(\mathbf{x})]$ is the Hessian matrix, formed by the second-order partial derivatives of the complete quadratic model.

The response surface design most commonly used is the central composite design (CCD), an arrangement consisting of a full-factorial or fractional, a set of center points, and, additionally, a group of extra levels called axial points. This arrangement's main advantage is that it can fit a quadratic model with the set of process parameters, maintaining the rotational arrangement. Rotatability is a property characterized by constant variation observed by the expected response for all experimental points located at the same axial distance [9]. In terms of optimization and process control, this property is extremely useful. The more external a solution adopted for the process, the less accurate will be the prediction of new values or an average.

As described above, the goal in testing was to define a machining operation setup excellent for internal and

Table 2 Mechanical properties of the substrate and coating for the developed carbide tools

Substrate		Coating	
Hardness (HV30)	1.6	Coating process	PVD arc evaporation
Density (g/cm ³)	14.45	Microhardness (HV 0.05)	2.3
Compressive strength (N/mm²)	6,250	Coefficient of friction against steel (dry)	0.4
Flexural strength (N/mm²)	4,300	Internal stress (GPa)	−2.5
Heat resistance (°C)	900	Max temp of application (°C)	600
Modulus of elasticity (kN/mm²)	580	Structure of coating	Monolayer
Grain size (mM)	0.8	Jacket color	Golden yellow

Table 3 Characteristics of cutting tools

Description	Inscribed circle (i.C), mm	Edge length (l), mm	Tool thickness (s), mm	Tip radius (r_ε), mm	Clearance angle (α)	Angle breaks the chip (γ)
Hexagonal	12	7	4.5	1.8	10°	3°
Square	12	12	4.5	1.3	10°	0°

external vertical turning, a setup that considered tool life (T), production rate (P_R), and machining cost per number (K_p). As shown in Table 5, taking a CCD to analyze the influence of tool feed and rotation of pack rings was the level considered.

Data from the vertical turning process of piston rings (shown in Table 6) were used to obtain the total machining time, production rate, and the machining cost per part. These responses of interest were obtained in the various cutting conditions suggested by the CCD array, using tool life (T) as a characteristic of output that was observed during the tests. The

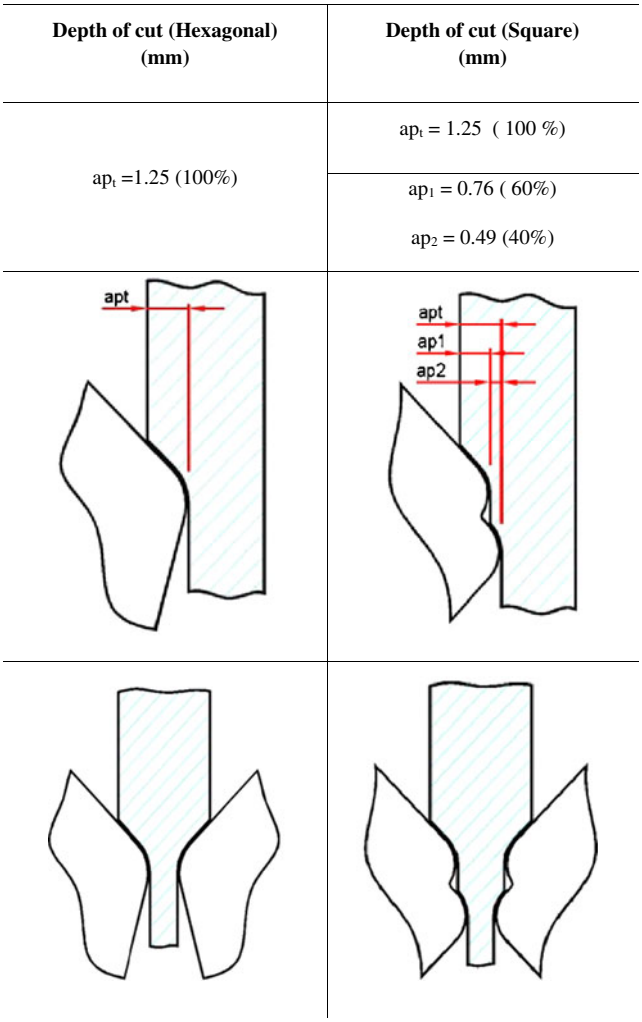

Fig. 4 Relationship between the geometries of the tool and the cutting depth

rate of production (P_R) and machining cost per part (K_p) were obtained, as suggested in Paiva et al. [13], from Eqs. 2, 3, and 4.

$$P_R = 60 \times T_t^{-1} \tag{2}$$

$$T_t = C_t + \left(t_a + t_s \frac{t_p}{Z}\right) + \left(\frac{C_t}{T} - \frac{1}{Z}\cdot\right) t_{ft} \tag{3}$$

$$K_p = \left(\frac{T_t}{60} - \frac{1}{Z}\right).(S_h + S_m) + \frac{C_t}{60}(S_h + S_m) + \frac{C_t}{T} \times \left[\left(\frac{V_{si}}{N_{fp}} + \frac{K_{pi}}{N_s}\right) + t_{ft}(S_h + S_m)\right] \tag{4}$$

The criteria for the end of tool life were based on the maximum flank wear VB_{max}=0.3 mm (Fig. 5a), the breakdown of the tool (Fig. 5b), and the chipping of the piston ring (Fig. 5c).

4 Modeling and optimization

The response surface models generally estimate the behavior of the average response characteristic. The equation of its variance, however, can be derived from the CCD array itself, using the principle of propagation of error [15]. In this case, the response variance, $\sigma^2_{\widehat{Y}(\mathbf{x})}$ can be obtained on the basis of a full quadratic model for the absolute values of residuals of $\widehat{Y}(\mathbf{x})$, $\sigma^2_{ei}\left[\widehat{Y}(\mathbf{x})\right]$. Whereas $\sigma^2_{ei}\left[\widehat{Y}(\mathbf{x})\right] = |\widehat{e}_i|$, the experimental variance $\left(\sigma^2_{\varepsilon_i}\right)$ obtained from the analysis of variance (ANOVA) of $\widehat{Y}(\mathbf{x})$, and adjusting the full quadratic model for residuals $\left(R_i^2\right)$, one can write:

$$\sigma^2_{\widehat{y}(\mathbf{x})} \cong \sigma^2_{ei}[\widehat{y}(\mathbf{x})] + \left(1 - R_i^2\right)\sigma^2_{\varepsilon_i} \tag{5}$$

Table 4 Factors and levels of full-factorial

Parameters	Symbol	Unit	Levels (Uncoded)	
			−1	1
Feed rate	f	mm×rot.$^{-1}$	0.32	0.38
Rotation	n	rpm	235	275
Tool geometry	G_t	–	Hexagonal	Square

Table 5 Levels of factors used in central composite design

Parameters	Symbol	Unit	Levels (Uncoded)				
			−1.41	−1	0	1	1.41
Feed rate	f	mm× rot.$^{-1}$	0.31	0.32	0.35	0.38	0.39
Rotation	n	rpm	227	235	255	275	283

For many problems, the optimal location of the point should be made using a constrained nonlinear algorithm. Thus, the solution must belong to the space experiment, such that $\mathbf{x}^T\mathbf{x} \leq \rho^2$. This constraint, however, can lead to optimal points belonging to the convex boundary of the region of solution. Although these points are feasible, the response variance increases with the expected departure from the center point of the optimal arrangement. To limit this increase in uncertainty, a constraint could be included that is related to the confidence interval for the mean, defined as $\widehat{y}(\mathbf{x_0}) \pm t_{\alpha/2,n-p} \times \sqrt{s\left[\mathbf{x_0^T}\left(\mathbf{X^TX}\right)^{-1}\mathbf{x_0}\right]}$ [3]. A compromise solution related to the increase of the processes must take into account the remoteness of the target media proposal and a simultaneous reduction of variance. In mathematical terms, this can be written as $\lambda_1[\widehat{y}_1(\mathbf{x}) - T]^2 + (1-\lambda_1)\sigma^2_{\widehat{y}(\mathbf{x})}$, where T is the target for the trait of interest and λ_1 is a weight denoting the relative importance between the mean and variance. Thus, to combine the functions obtained experimentally with the algorithms for solving the optimization problem, we can write:

Table 6 Technical and economic process variables

Parameters	Symbols	Values
Tool life	T	From CCD
Batch of parts (units)	Z	15,000
Cutting time (min)	C_t	Calculated
Secondary time (min)	T_s	0.003
Approximation and removal tool time (min)	T_a	0.008
Setup time (min)	T_p	25
Tool change time (min)	T_{ft}	2
Unproductive time (min)	t_l	0.0125
Cost + machinery operator (US $/h)	(S_m+S_h)	80
Cost of the tool holder (internal + external) (US $)	V_{si}	250
Average life of tool holders (external and internal), edges	N_{fp}	2,400
Cost of the square insert (internal + external) (US $)	Kpi qd.	64
Number of edges of square insert	Ns qd.	4
Cost of hexagonal insert (foreign + domestic) (US $)	Kpi hx.	40
Number of edges of hexagonal insert	Ns hx.	6
Path forward (mm)	Lf	1.95
Initial diameter of the part (mm)	D_i	81.35
Final part diameter (mm)	D_f	78.98
Average final part diameter (mm)	D_m	80.165

$$\begin{aligned}
&\text{Minimize} \quad f(\mathbf{x}) = \lambda_1[\widehat{y}_1(\mathbf{x}) - T]^2 + (1-\lambda_1)\sigma^2_{\widehat{y}(\mathbf{x})} \\
&\text{Subject to :} \quad g_i(\mathbf{x}) \leq 0 \\
&\qquad \mathbf{x}^T\mathbf{x} \leq \rho^2 \\
&\qquad \mathrm{Var}[\widehat{y}(\mathbf{x})] \leq \varepsilon \\
&\qquad \widehat{y}(\mathbf{x_0}) + t_{\alpha/2,n-p} \times \sqrt{s^2\left[\mathbf{x_0^T}\left(\mathbf{X^TX}\right)^{-1}\mathbf{x_0}\right]} \leq Ub \\
&\qquad \widehat{y}(\mathbf{x_0}) - t_{\alpha/2,n-p} \times \sqrt{s^2\left[\mathbf{x_0^T}\left(\mathbf{X^TX}\right)^{-1}\mathbf{x_0}\right]} \geq Lb
\end{aligned} \tag{6}$$

With: $\widehat{y}(\mathbf{x}) = b_0 + \left[\nabla f(\mathbf{x})^T\right] + \left\{\frac{1}{2}\mathbf{x}^T[\nabla^2 f(\mathbf{x})]\mathbf{x}\right\}$

The optimization system of Eq. 6 can be solved using the algorithm of the GRG. The GRG is one of the most robust and efficient methods of constrained nonlinear optimization [6]. The algorithm assumes the partition of the original variables into basic ($\boldsymbol{Z}$) and non-core ($\boldsymbol{Y}$) such that $F(X)=F(Z,Y)$ and $h(X)=h(Z,Y)$. To meet the optimality condition requires that $dh_j(X)=0$, making $A = \nabla_z h_j(X)^T$ e$B = \nabla_Y h_j(X)^T$, then $dY=-B^{-1}AdZ$. Thus, the GRG can be written as:

$$G_R = \frac{d}{dZ}F(X) = \nabla_z F(X) - \left[B^{-1}A\right]^T \nabla_Y F(X)^T \tag{7}$$

The search direction is $S_X = \left[-G_R \quad dY\right]^T$. For iterations, $X^{k+1} = X^k + \alpha S^{k+1}$ should be used, verifying at each step whether X^{k+1} is feasible and $h(X^{k+1})=0$. Then, just solve $F(X)$ written in terms of α, using a one-dimensional search algorithm, like Newton's method.

Once we model the main features of the process's quality and productivity, we can apply it to the previously proposed optimization system.

5 Results and discussion

Taking into account the results obtained for the tool life (T) with factorial arrangement 2^3, a statistical analysis was performed using Minitab® 15 software, obtaining a model for tool life (T). Table 7 presents the results obtained in experiments with the full-factorial.

The statistical analysis showed that all main effects and interactions were significant (P-values <5%), with adjusted R^2 equal to 97.81%. Figure 6 presents an analysis of the main factors on the tool life.

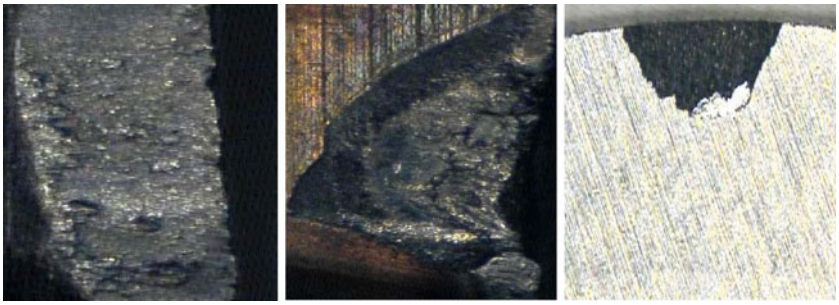

(a) Flank wear (b) Tool Breakage (c) Chipped Piston Ring

Fig. 5 Criteria for end of cutting tool life. **a** Flank wear, **b** tool breakage, **c** chipped piston ring

According to this analysis, the most significant factor for increasing tool life is the tool's geometry, followed by rotation, and then feed. In the vertical turning of martensitic gray cast iron, the special square tool showed the best performance, thanks to its staggered cutting edge. This cutting edge splits the removal of material during the cutting operation and the cutting edge is strengthened by two radii of 1.3 mm each, leading to increased tool life. A total of 60% of the material is removed by the first cutting edge; the second cutting edge removes the remainder. Martensitic cast iron, with its particularly irregular and extremely abrasive surface, has an uncommonly deleterious effect on tools; this effect can be ameliorated by the special square-shaped tool's geometry and its staggered two tip radii of 1.3 mm each.

Since the model shows interactions among the main factors, we cannot complete the study by analyzing only their main effects on tool life.

5.1 Full quadratic models

Having better defined the geometry of the tool, we chose to explore the parameters of cutting speed and feed using a CCD (Table 8). In this phase of the work, tool life was also discussed considering the production rate and the machining cost per part. All these properties are obtained using the special geometry of the staggered square.

Table 7 Full-factorial design for tool life

Experiment number	f (mm/rot.)	n (rpm)	G_t	T (mm)
1	0.32	275	Hexagonal	400
2	0.32	235	Square	2,202
3	0.38	275	Hexagonal	1,001
4	0.32	235	Hexagonal	1,351
5	0.32	275	Square	1,902
6	0.38	235	Hexagonal	701
7	0.38	275	Square	1,802
8	0.38	235	Square	3,053

Table 9 presents the ANOVA, significance of the terms of the models, and an analysis of the residue of the responses studied. Aside from the feed rate to tool life and rotation to machining cost per part, the main effects as well as the interactions were significant for the models. Since for all the answers the adjusted R^2 values were above 90%, the results show that the models demonstrated excellent fit. Although some terms are not meaningful in isolation, excluding them hampers the ability to explain the model. Consequently, an increased experimental variance was found to justify adopting them in this study. Residual analysis was performed to compare with normal tool life, production rate, and cost.

Figure 7 shows the response surfaces for the tool life and the cost of the process and describes the behavior of the interactions between the cutting parameters for each response of interest. It can be seen in Fig. 7a that the greatest tool life occurred at intermediate rates of feed and rotation, i.e., at intermediate levels of feed rate and cutting times. Due to the extremely abrasive surface of martensitic cast iron, a reduction in cutting time moderately favors an increase in tool life. In Fig. 7b, we can see that a high feed rate but lower RPM obtains a lower machining cost per part. Unlike T and K_p, the process is productive (Fig. 8) only at the highest feed and rotation speeds.

Considering the individual optimization from the quadratic models obtained and using the GRG algorithm, we can observe those results shown in Table 10.

Given the conflicting nature of the responses of interest, we can conclude that for the proper functioning of the process individual optimization may not meet all the necessary requirements. It was possible, however, to identify which values could be used as targets of response variables during optimization for multiple prioritizations.

Thus, according to the equation proposed in the system of Eq. 3 and considering the results obtained in the individual optimization of the three responses of

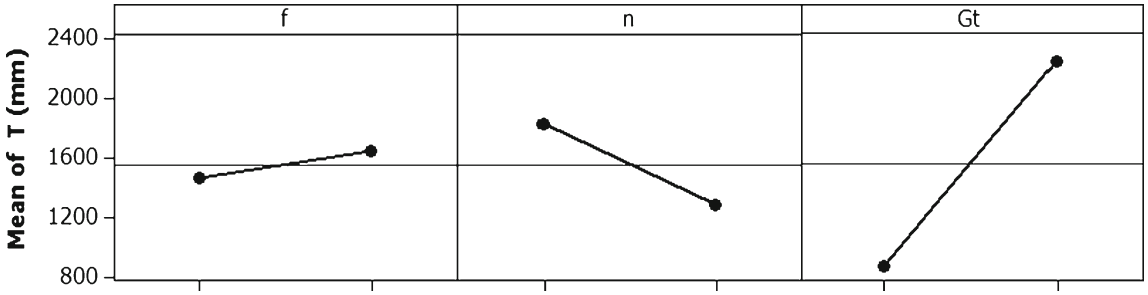

Fig. 6 Main effects for tool life

interest, we can propose the following system for simultaneous optimization:

$$\begin{aligned}
&\text{Min} \quad f(\mathbf{x}) = \lambda_1 \left[\widehat{P}_{\mathrm{r}}(\mathbf{x}) - T\right]^2 + (1-\lambda_1)\widehat{\sigma}^2_{\widehat{P}_{\mathrm{r}}(\mathbf{x})} \\
&\text{Subject to :} \quad \widehat{T}(\mathbf{x}) \geq 2,450 \\
&\qquad \widehat{K}_{\mathrm{p}}(\mathbf{x}) \leq 0.038 \\
&\qquad \mathbf{x}^T\mathbf{x} \leq 2.00 \\
&\qquad \mathrm{Var}[\widehat{y}(\mathbf{x})] \leq 2.1 \\
&\qquad \widehat{T}(\mathbf{x_0}) + \left\{ t_{\alpha/2,n-p} \times \sqrt{s_1^2 \left[\mathbf{x^T_0}\left(\mathbf{X^T X}\right)^{-1}\mathbf{x_0}\right]} \right\} \leq 2,700 \\
&\qquad \widehat{T}(\mathbf{x_0}) - \left\{ t_{\alpha/2,n-p} \times \sqrt{s_1^2 \left[\mathbf{x^T_0}\left(\mathbf{X^T X}\right)^{-1}\mathbf{x_0}\right]} \right\} \geq 2,200 \\
&\qquad \widehat{P}_{\mathrm{r}}(\mathbf{x_0}) + \left\{ t_{\alpha/2,n-p} \times \sqrt{s_2^2 \left[\mathbf{x^T_0}\left(\mathbf{X^T X}\right)^{-1}\mathbf{x_0}\right]} \right\} \leq 1,904 \\
&\qquad \widehat{P}_{r}(\mathbf{x_0}) - \left\{ t_{\alpha/2,n-p} \times \sqrt{s_2^2 \left[\mathbf{x^T_0}\left(\mathbf{X^T X}\right)^{-1}\mathbf{x_0}\right]} \right\} \geq 1896
\end{aligned} \tag{8}$$

Where $t_{(0.025;\ 7)}$=2.364, $s_1^2 = 13.38$, $s_2^2 = 35765.00$, λ_1= 0.8, and $(\mathrm{X^T X})^{-1}$ is determined as below:

$$\left(\mathbf{X^T X}\right)^{-1} = \begin{bmatrix} 0.200 & 0.000 & 0.000 & -0.100 & -0.100 & 0.000 \\ 0.000 & 0.125 & 0.000 & 0.000 & 0.000 & 0.000 \\ 0.000 & 0.000 & 0.125 & 0.000 & 0.000 & 0.000 \\ -0.100 & 0.000 & 0.000 & 0.144 & 0.019 & 0.000 \\ -0.100 & 0.000 & 0.000 & 0.019 & 0.144 & 0.000 \\ 0.000 & 0.000 & 0.000 & 0.000 & 0.000 & 0.250 \end{bmatrix}$$

Figure 9 shows the overlap of the different objective functions and constraints and the feasible region for the problem. For the GRG algorithm to be applied in solving the optimization system, we must provide a feasible starting point. Starting, therefore, with the point f=0.35 mm/rev and n=271 rpm, after eight iterations (Fig. 10), we obtained an optimal located at f=0.37 mm/rev and n=264 rpm. Table 11 shows the values of the three response variables obtained in this condition and a comparison made with respect to the hexagonal tool.

Table 8 CCDs for tool life (T), production rate (P_{R}), and cost (K_{p})

Experiment number	f (mm/rot.)	n (rpm)	T (mm)	P_{R} (pc/h)	K_{p} ($/pc)
1	0.32	235	2,102	1,523	0.04686
2	0.38	235	2,853	1,712	0.03682
3	0.32	275	1,802	1,677	0.04474
4	0.38	275	1,501	1,847	0.04413
5	0.31	255	1,652	1,555	0.05019
6	0.39	255	1,802	1,813	0.04117
7	0.35	227	2,853	1,588	0.04047
8	0.35	283	1,952	1,807	0.03985
9	0.35	255	3,153	1,714	0.03562
10	0.35	255	3,003	1,713	0.03620
11	0.35	255	3,303	1,716	0.03509
12	0.35	255	2,703	1,709	0.03755
13	0.35	255	2,853	1,711	0.03684

Table 9 Analysis of significance for individual terms of models and ANOVA

Terms	T (mm)	P_{R} (pc/h)	K_{p} ($/pc)
Constant	*3003*	*1713*	*0.03626*
f	83	*90*	*-0.00293*
n	*-366*	*75*	0.00054
f^2	*-638*	*-15*	*0.00476*
n^2	*-300*	*-8*	*0.00200*
$f \times n$	*-263*	*-5*	*0.00236*
MSE		*12.9*	
P-value			
Regression (full quadratic)	0.000	0.000	0.000
Lack of fit	0.926	0.136	0.279
R^2 (adj.), %	91.10	99.90	94.30
Normality of residuals	0.600	0.511	0.552

Values in italics represent significant terms of the full quadratic model (P-value <5%)

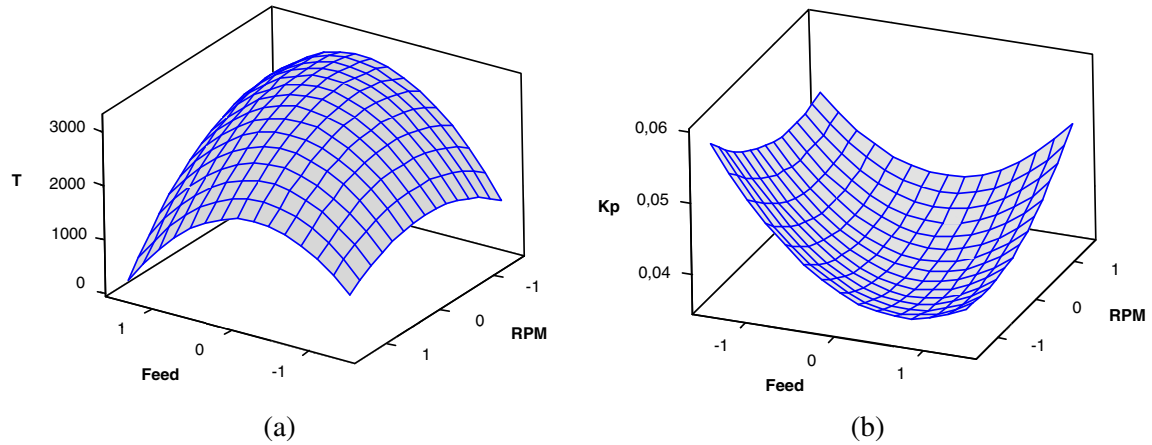

(a) (b)

Fig. 7 **a**, **b** Effect of interaction between feed and rotation on T and K_p

5.2 Confirmation runs

Having defined the optimum cutting conditions for the vertical turning of martensitic cast iron piston rings, we confirmed the mathematical results. We tested 75 times the optimal condition grouped in 15 samples of size $n=5$. Noise conditions used during the machining process of the confirming trial were identical to those adopted during data collection. After testing was completed, the value predicted by the model lay in the range of 95% confidence interval established for the confirmation experiments (Fig. 11). Such a value reveals that the proposed model, experimentally obtained through DOE, helps improve the machining process.

Changes in the levels of factors positively impacted tool life, production rate, and cost of machining. The improvements in the machining process of the martensitic cast iron piston rings can be explained by the changes to the cutting parameters and tool geometry.

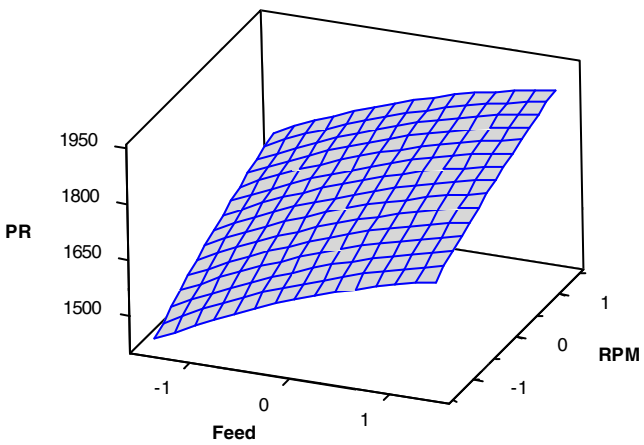

Fig. 8 Response surface for yield (P_R)

The contact time between the workpiece and tool was reduced by increasing the feed rate to 15.63%. Reducing this contact time contributes to reduced machining time and longer tool life, increasing the rate of production of piston rings. Rotation was increased by 12.34%, contributing to a higher spindle speed, reducing machining time, and favoring the rate of production. Last but not least, the change in geometry of the cutting tool contributed significantly to the success of this study. The development of the special square-shaped geometry gave rise to the improved tool life and machining conditions obtained in this study.

6 Conclusion

Depending on the results obtained, one can conclude the following about the study of the optimization of the vertical turning of dual piston rings of martensitic cast iron:

1. Tool life increased significantly, a fact explained by the difference in the cutting geometry and the interaction of cutting parameters, feed, and rotation. The special geometry of the square tool showed better performance due to its design of two cutting edges, staggered. The interaction between the cutting parameters decreased

Table 10 Points of individual optimals (T, P_R, and K_p)

	T (mm)	P_R (Parts/h)	K_p ($/Part)
$\hat{y}_i$	3,140	1,850	0.035
f	0.36	0.41	0.37
n	227	294	240

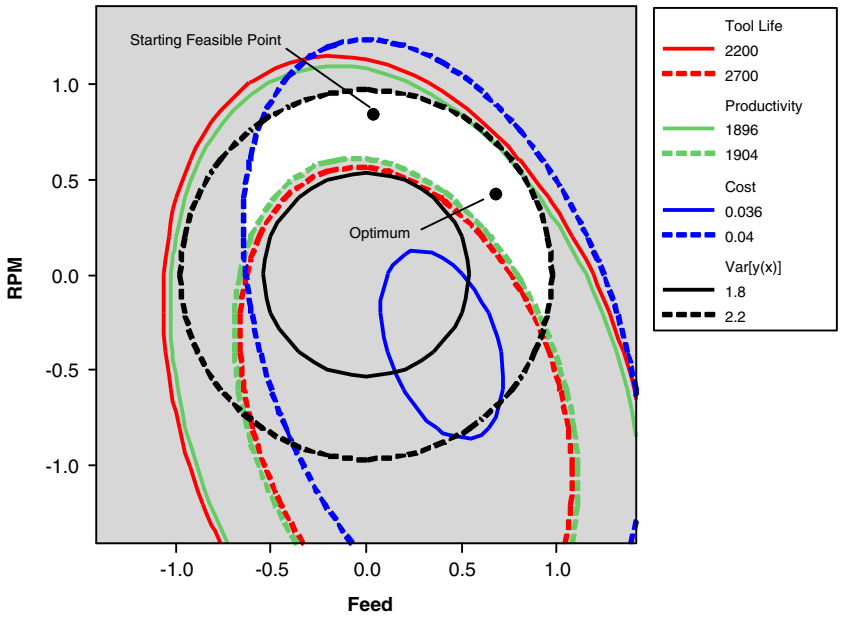

Fig. 9 Point of optimization for common responses (T, P_R, and $K_{p)}$

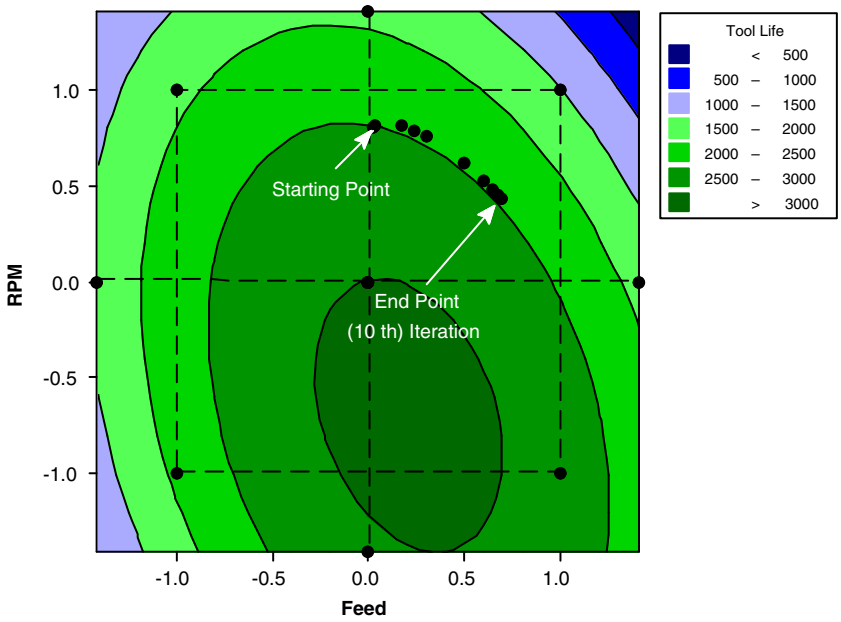

Fig. 10 Iterations of GRG in the plane of tool life

Table 11 Comparison between optimal versus previous condition

Parameters	Previous	Optimized	Previous	Optimized
f (mm/rot.)	0.32	0.37		0.67
n (rpm)	235	264		0.46
G_t	Hexagonal	Square	Lower bound (95%)	Upper bound (95%)
T (mm)	1,351	2,450	2,243	2,657
P_R (pc/h)	1,451	1,798	1,795	1,802
K_p ($/pc)	0.059	0.038	0.037	0.039

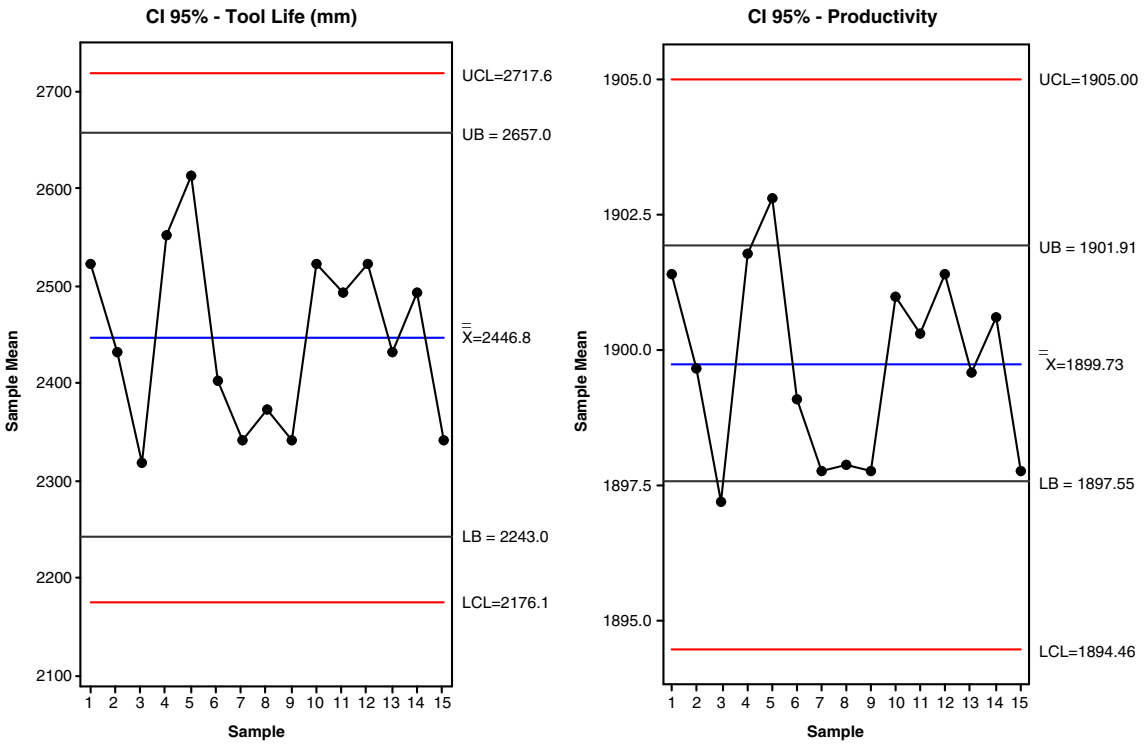

Fig. 11 X-bar control chart with 95% confidence intervals for confirmation runs

the contact time between the workpiece and tool, contributing to increased tool life.

2. The production rate was increased due to optimization of process parameters (feed, speed, and tool geometry), which contributed to a lower total machining time per manufactured part and a longer tool life. The optimized condition, where the feed rate (inside and outside) was increased by 15.62%, reduced the total machining time per part, thus increasing the rate of production.
3. The reduction of machining cost per part was realized because of the sum of the benefits from better cutting tool geometry and cutting parameters optimized for the machining of martensitic gray cast iron in vertical turning operations.
4. For the responses studied, the results were significant—an increase of 81.35% in tool life, of 23.91% in production rate, and a decrease of 35.50% in machining cost per part.
5. The optimization of the turning machine based on the design of experiments combined with the GRG algorithm, available in the application of Solver® optimization, forms a very useful approach to modeling machining conditions.
6. After being applied on a real scale by a piston rings' manufacturer, the optimal condition obtained with the present proposal was proved to be stable, predictable, and under control. The proposed confidence intervals were supported.

Even considering the quality of results of this approach, these findings cannot be extrapolated to different materials, tools, or machine tools and are valid only for the levels adopted. The approach, however, can be recommended as a means to optimize any manufacturing process.

Acknowledgements Thanks to MAHLE Engine Components of Brazil, FECIAL, CNPq, and FAPEMIG for the support they gave to this work.

References

1. Al-Ahmari AMA (2007) Predictive machinability models for a selected hard material in turning operations. J Mater Proc Technol 190(1–3):305–311
2. Courbon C, Kramar D, Krajnik P, Pusavec F, Rech J, Kopac J (2009) Investigation of machining performance in high-pressure jet assisted turning of Inconel 718: an experimental study. Int J Mach Tools Manuf 49:1114–1125
3. Del Castillo E (2007) Process optimization—a statistical approach, 1st edn. Springer, New York, pp 32–87
4. Hejazi MM, Divandari M, Taghaddos E (2009) Effect of copper insert on the microstructure of gray iron produced via lost foam casting. Mater Des 30(4):1085–1092
5. Horng JT, Liu NM, Chiang KT (2008) Investigating the machinability evaluation of Hadfield steel in the hard turning with Al_2O_3/

TiC mixed ceramic tool based on the response surface methodology. J Mater Proc Technol 208(1–3):532–541
6. Köksoy O, Doganaksoy N (2003) Joint optimization of mean and standard deviation using response surface methods. J Qual Technol 35(3):237–334
7. Kurt M, Bagci E, Kaynak Y (2009) Application of Taguchi methods in the optimization of cutting parameters for surface finish and hole diameter accuracy in dry drilling processes. Int J Adv Manuf Technol 40(5–6):458–469
8. Lalwani DI, Mehta NK, Jain PK (2008) Experimental investigations of cutting parameters influence on cutting forces and surface roughness in finish hard turning of MDN250 steel. J Mater Proc Technol 206(1–3):167–179
9. Montgomery DC (2009) Design and analysis of experiments, 7th edn. Wiley, New York, pp 418–445
10. Myers RH, Montgomery DC (2002) Response surface methodology—process and product optimization using designed experiments, 2nd edn. Wiley, New York, pp 235–286
11. Nalbant M, Gokkaya H, Sur G (2007) Application of Taguchi method in the optimization of cutting parameters for surface roughness in turning. Mater Des 28(4):1379–1385
12. Noordin MY, Venkatesh VC, Sharif S, Elting S, Abdullah A (2004) Application of response surface methodology in describing the performance of coated carbide tools when turning AISI 1045 steel. J Mater Proc Technol 145(1):46–58
13. Paiva AP, Ferrreira JR, Balestrassi PP (2007) A multivariate hybrid approach applied to AISI 52100 hardened steel turning optimization. J Mater Proc Technol 189(1–3):26–35
14. Pereira AA, Boehs L, Guesser LW (2006) The influence of sulfur on the machinability of gray cast iron FC25. J Mater Proc Technol 179(1–3):165–171
15. Plante RD (2001) Process capability: a criterion for optimizing multiple response product and process design. IIE Trans 33:497–509
16. Pradhan SK, Nayak BB, Mohapatra BK, Mishra BK (2007) Micro Raman spectroscopy and electron probe microanalysis of graphite spherulites and flakes in cast iron. Met Mater Trans 38(10):2363–2370
17. Reddy NSK, Rao PV (2005) Selection of optimum tool geometry and cutting conditions using a surface roughness prediction model for end milling. Int J Adv Manuf Technol 26(11–12):1202–1210
18. Sarma DK, Dixit US (2007) A comparison of dry and air-cooled turning of grey cast iron with mixed oxide ceramic tool. J Mater Proc Technol 190(1–3):160–172
19. Souza JVC, Nono MCA, Ribeiro MV, Machado JPB, Silva OMM (2009) Cutting forces in turning of gray cast iron using silicon nitride based cutting tool. Mater Des 30(7):2715–2720
20. Wang W, Jing T, Gao Y, Qiao G, Zhao X (2007) Properties of a gray cast iron with oriented graphite flakes. J Mater Proc Technol 182(1–3):593–597